Quantitative Bathymetric Models for Late Quaternary Transgressive-Regressive Cycles of the Po Plain, Italy

Jacalyn M. Wittmer,[1,*] *Troy A. Dexter,*[2] *Daniele Scarponi,*[3] *Alessandro Amorosi,*[3] *and Michał Kowalewski*[2]

1. Department of Geology, University of Illinois at Urbana-Champaign, Champaign, Illinois 61820, USA; 2. Department of Natural History, Florida Museum of Natural History, University of Florida, Gainesville, Florida 32611, USA; 3. Dipartimento di Scienze Biologiche, Geologiche e Ambientali, University of Bologna, Bologna 40126, Italy

ABSTRACT

In marine settings, quantitative bathymetric models can be developed using various water depth proxies, including epibiont distribution, sedimentologic features, and the distribution of benthic taxa in time and space. Here, the late Quaternary bathymetric history of the Po coastal plain (Italy) has been reconstructed using mollusk samples from a network of 16 cores. Multiple analytical approaches have been applied in a comparative fashion. A direct ordination approach was used to estimate sample bathymetry using weighted averaging of genera with known preferred depth. Weighted averaging carries an advantage of analytical simplicity and produces direct ordination models expressed in environmentally meaningful units. Indirect ordination methods, based on depth estimates developed using posteriori-calibrated ordination strategies (correspondence and detrended correspondence analysis calibrated against present-day bathymetric data), yielded results consistent with weighted averaging. Regardless of the choice of analytical methods, mollusk assemblages yielded bathymetric proxies congruent with independent sequence stratigraphic interpretations derived previously for both Late Pleistocene and Holocene transgressive-regressive cycles. The mollusk-derived proxies quantify spatial bathymetric gradients across the basin and local trends in absolute water depth in response to relative changes in sea level. However, for cores located in the most proximal part of the basin, mollusk-based ordinations failed to provide viable estimates due to inclusion of mixed marine and nonmarine mollusk faunas and scarcity of fossiliferous horizons necessary for adequate quantitative sampling. The multiple analytical approaches cross evaluated in this study consistently suggest that high-resolution quantitative bathymetric estimates can be derived for mollusk samples independent of stratigraphy for fully marine settings. When applied simultaneously to both samples and taxa, these approaches provide a viable strategy for quantifying stratigraphic and paleontological patterns and enhancing interpretations of basin-scale depositional systems.

Online enhancements: supplementary figures.

Introduction

The field of stratigraphic paleobiology has progressed considerably in the past 20 years: an increasing integration of sequence stratigraphy and quantitative paleobiology has enhanced our ability to explore jointly stratigraphic and paleobiologic patterns in time and space (Cisne and Rabe 1978; Brett 1995; Holland 1995, 2000; Patzkowsky and Holland 1996; Holland et al. 2001; Scarponi and Kowalewski 2004; Holland and Patzkowsky 2007; Hendy 2013). In particular, fossil-derived patterns provide us with an independent assessment of environmental changes potentially refining and cross testing sedimentary-based interpretations and models (Holland 2000; Miller et al. 2001; Peters 2005, 2006; Peters and Heim 2010; Patzkowsky and Holland 2012; Scarponi et al. 2014).

It has been shown that taxonomic composition of assemblages at the basin scale correlate to environmental gradients such as water depth (bathymetry), salinity, energy, substrate, oxygen, and nutrient levels (Funder et al. 2002; Ceregato et al. 2007; Patzkowsky and Holland 2012 and refer-

Manuscript received January 24, 2014; accepted June 21, 2014; electronically published November 12, 2014.

* Author for correspondence; e-mail: jwittm2@illinois.edu.

[The Journal of Geology, 2014, volume 122, p. 649–670] 0022-1376/2014/12206-0002$15.00. DOI:10.1086/677901

ences therein). Also in ecological studies, bathymetry, which tends to correlate with many other environmental variables, is commonly invoked to describe faunal gradients (e.g., Carney 2005; Olabarria 2006; Konar et al. 2008; Smale 2008; Zuschin et al. 2014) and has been demonstrated to be an effective tool for delineating past biotic changes (Holland 2005; Hendy and Kamp 2007). However, other variables can also leave an important or even overriding imprint in the geological record (Lafferty et al. 1994; Redman et al. 2007; Bush and Brame 2010; Huntley and Scarponi 2012; Amorosi et al. 2014*b*). The focus of this article is to evaluate water depth as an environmental variable and assess its importance in controlling spatial and temporal ecological patterns within a sequence stratigraphic context.

Changes in water depth along and across sedimentary successions can be estimated using various strategies. Sedimentologic features such as grain size, bedding, and sedimentary structures are frequently employed to semiquantitatively reconstruct bathymetric gradients (Dattilo 1996; Zong and Horton 1999; Holland and Patzkowsky 2007). Epibiont and microendolith distribution can also be used to identify the photic zone (Smrecak 2008; Hannon and Meyer 2014). Last, macrobenthic marine invertebrates can be used to develop numerical bathymetric-based interpretations of sedimentary successions by means of multivariate ordination analyses (e.g., Cisne and Rabe 1978; Holland et al. 2001; Scarponi and Kowalewski 2004; Scarponi and Angeletti 2008). This study focuses primarily on the last of these approaches.

Here, we examine the latest Quaternary (<130 k.yr. ago) succession of the Po coastal plain, which is part of an active sedimentary basin that is well understood in terms of its sequence stratigraphic architecture and recent sea-level history.

Quaternary successions offer a powerful advantage for exploring paleoecological patterns within their sequence stratigraphic framework because samples are dominated by extant taxa with well-understood biology, ecology, biogeography, and taxonomic/phylogenetic affinity. Such paleoecological data can be calibrated against estimates derived from modern environments and provide us with a direct means for testing the accuracy and strength of quantitative paleoecological strategies for resolving depositional environments and outline sequence stratigraphic interpretations of sedimentary successions.

In a pilot study assessing the latest Quaternary fossiliferous marine sequences of the Po coastal plain (Italy), Scarponi and Kowalewski (2004) documented a bathymetric gradient from three cores representing a two-dimensional cross section oblique to the regional depositional profile. These incipient data indicated that paleoecological data coupled with ecological estimates from modern environments can provide a powerful tool for joint stratigraphic-paleobiologic analyses of Quaternary sedimentary basins. Building on this initial analysis, we undertake here a comprehensive examination of the late Quaternary successions of the southeastern Po coastal plain using a three-dimensional network of cores distributed along and across the depositional profile of the basin. From these cores, we assess the value of an integrated analysis of sequence stratigraphic and quantitative paleoecological patterns. The aim of this project is threefold: (1) to determine the viability of paleoecological data for deriving quantitative estimates of water depth, (2) to compare different analytical strategies for deriving such bathymetric estimates, and (3) to explore the informative value of this approach for quantifying bathymetric gradients and enhancing stratigraphic interpretations of sedimentary successions.

Geological Setting

The Po Plain, situated in northern Italy, is the emerged surface of a relatively large foreland basin bounded by the Alps to the north and the Apennines to the south (i.e., Po Basin; fig. 1*A*). Its rock record includes a thick succession of strongly deformed Pliocene and less tectonically disturbed Pleistocene to Holocene deposits (Pieri and Groppi 1981). The Po Basin geometry has been investigated in detail during past decades through the integration of seismic studies and well-log interpretations aimed at the exploration of natural resources. These studies have led to internal subdivision of the Pliocene-Quaternary succession of the Po Basin into a series of third-order depositional sequences. The basal unconformities are well developed at the basin margin, where they mark phases of dramatic basin reorganization generally related to phases of intense tectonic activity (e.g., Gunderson et al. 2011). These unconformities grade basinward into correlative conformable surfaces.

The uppermost third-order depositional sequence of the Po Basin consists of Middle Pleistocene to Holocene deposits. On the basis of magnetostratigraphic data, its lower boundary (at 0.87 Ma, according to Muttoni et al. 2007) is close to the Matuyama-Brunhes reversal. This depositional se-

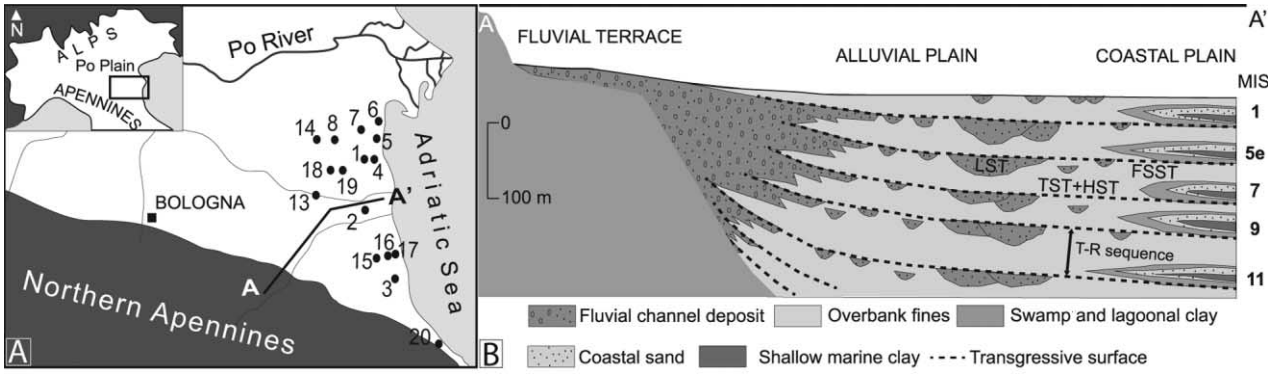

Figure 1. Map of the study area (*A*) and geological cross section (*B*) of the uppermost deposits of the southern Po Plain (from Amorosi et al. 2014*a*, 2014*b*). *A*, Localities indicated by black circles. *B*, Geological cross section along a plane defined by A to A′, with the cores occurring below sea level because the region is an abandoned Po delta lobe subject to sediment compaction and subsidence. Numbers on the right indicate the marine isotope stage (MIS) for the lower part of that sequence. Only the five most recent fourth-order depositional cycles are shown. FSST = falling stage systems tract; HST = highstand systems tract; LST = lowstand systems tract; T-R = transgressive-regressive; TST = transgressive systems tract. Scale: 1:50,000.

quence consists of a series of eight vertically stacked, higher-order (fourth-order) depositional cycles, which exhibit distinctive transgressive-regressive trends and reflect a clear glacio-eustatic-induced cyclicity (Amorosi et al. 1999; fig. 1*B*).

Detailed sedimentologic and paleobiologic core-based analyses integrated in a well-resolved chronostratigraphic framework (amino acid, radiocarbon, and pollen) documented the paleogeographic and paleoclimatic development of the Po coastal plain during the latest Quaternary and its marked relationship with the most recent Quaternary eustatic sea-level changes (fig. 1*B*). Two prominent stratigraphic markers, corresponding to characteristic wedge-shaped coastal sand bodies with very similar internal architecture, are recorded beneath the modern coastal plain at 0–30-m and 95–120-m core depth intervals, respectively. These nearshore to shallow-marine packages are separated by a thick succession of alluvial deposits. Recent studies (e.g., Amorosi et al. 2004) have documented that these coastal bodies were deposited under predominantly glacio-eustatic (100 k.yr.) control during the last two major transgressive pulses and subsequent sea-level highstands, corresponding to marine isotope stage (MIS) 5e and 1, respectively (fig. 1*B*). In contrast, coastal to alluvial sedimentation took place in a subsiding setting, during the long phase of sea-level fall between MIS 5d and 2. Stratigraphic architecture recovered from the deepest parts of the studied cores suggests phases of episodic sedimentation and widespread erosion in alluvial settings corresponding to—and/or immediately post-dating—the penultimate glacial maximum (i.e., MIS 6).

Marine isotope stratigraphy is a method of determining the relative ages of marine sediments on the basis of measurement of isotopic ratios of stable isotopes of ^{16}O and ^{18}O in carbonate and phosphate shells of microorganisms. The O^{16}/O^{18} ratio measured in microfossil shells generally approximates the oxygen isotope ratio of the water in which those shells grew. Consequently, oxygen isotopes estimated from microfossil tests can be used as a proxy for ocean temperature and ice volume. When ice caps build up as a consequence of climatic cooling phases, the ^{16}O isotope is preferentially captured in the continental ice and the ocean water becomes enriched in ^{18}O. Because ice caps and temperature are both driven by Milankovitch climatic oscillations, oxygen isotope sequences can be subdivided into stages (MIS) and used to refine the late Cenozoic time scale (Emiliani 1955, 1966; Gibbard 2007). The MIS boundaries are defined as midpoints between maxima and minima and are assumed to be globally isochronous. The MIS time intervals can be cross correlated directly with terrestrial sequences using direct dating techniques. For the Po coastal plain successions, direct correlation was achieved by direct dating (^{14}C) and the use of pollen markers.

Rapid climatic change (and subsequent sea-level rise) following the late Middle Pleistocene glacial maximum induced a rapid landward migration of

the depositional environments. This landward shift of the shoreline is recorded by superposition of the lower wedge-shaped coastal body onto the glacial continental deposits. In sequence stratigraphic terms, this unit corresponds to transgressive systems tract (TST) and highstand systems tract (HST) deposits related to MIS 5e.

The overall eustatic sea-level fall documented between ~120 and ~30 ka (MIS 5e/5d transition to MIS 3/2 transition) induced a forced and generalized downward shift of facies, documented in the study area by coastal (MIS 5e–5a) to alluvial plain (MIS 4–3) bodies of variable thickness bounded by clustered erosional surfaces (falling-stage systems tract [FSST]; Amorosi et al. 2004). Paleosols are also recorded (especially landward), suggesting fluvial entrenchment during falling sea level. However, lesser climatic changes and higher frequency pulses punctuated the long-lived erratic FSST and are recorded in the sedimentary succession by relatively continuous, peat-enriched deposits representing primarily lagoon (MIS 5c) to wetland (MIS 5a and 3) depositional settings (Amorosi et al. 2004).

The sedimentary expressions of the last glacial maximum (LGM) and the early phases of the post-LGM transgression (MIS 2) are generally scarce. Channel entrenchment at the MIS 3/2 transition led to widespread paleosol development in the study area (Amorosi et al. 2014*a*), whereas the active lowstand sedimentation (lowstand systems tract [LST]) was restricted to the adjacent incised valleys. Consequently, in interfluve position the overlying transgressive surface tends to merge with the sequence boundary.

The ensuing postglacial dynamics (ca. MIS 1) are manifested in a well-studied and chronologically framed wedge-shaped coastal body (depicting a transgressive-regressive cycle) that shows striking affinity with the Late Pleistocene (MIS 5e) one. Hence, the transgressive surfaces of MIS 5e and 1 age, which mark facies shifts in more distal parts of the basin while recording important sedimentary hiatuses farther inland (see Amorosi et al. 2003 for detailed information), are considerably easier to identify than the other key sequence stratigraphic surfaces.

The lower transgressive deposits record the rapid landward migration of a lagoon-barrier-estuary system, giving way to widespread marginal marine sedimentation in the eastern part of the study area. During the early stages of transgression, the backstepping migration of coastal facies resulted in the development of a characteristic wave ravinement surface, usually enriched in fossils, that divides the transgressive deposits into two wedges thickening in opposite directions (fig. 1 in Scarponi and Kowalewski 2004). Across the investigated area, the ravinement surface marks the boundary between the lower TST (marsh and inlet facies associations) and the upper TST (lower shoreface and offshore transition deposits).

During the late phase of fast sea-level rise, the shoreline shifted up to ~20/30 km west of its present-day position, recording the maximum marine ingression. This stratigraphic interval, developed at peak transgression, includes the maximum flooding surface (MFS). In cores, the MFS marks the turnaround from a deepening-up to a shallowing-up tendency. This surface has no obvious physical expression and has been identified uniquely on the basis of subtle paleontological features (Scarponi and Kowalewski 2004; Amorosi et al. 2008 and references therein).

From the middle Holocene onward, the reduced rate of eustatic sea-level rise induced the basinward migration of coastal depositional environments. The basinward shift of facies took place at progressively increasing rates (e.g., Amorosi et al. 2008; Scarponi et al. 2013), as documented by the transition from an aggradational to a distinctive progradational stacking pattern of facies. At relatively distal locations, progradation is expressed in marine deposits by shallowing-upward (i.e., offshore to nearshore or prodelta to delta front) deposits. Landward, delta plain and coastal plain deposits record a dynamic environmental mosaic of wetlands, fluvial channels, and partly emerged lands, where autogenic (e.g., channel avulsion, differential compaction, delta lobe abandonment) and allogenic (higher-frequency climatic oscillation) signals are tangled and difficult to decouple.

In addition, changes in sediment supply, frequency of depositional environments, and net accumulation rates are tied closely to the temporal resolution of the fossil assemblages. A recent study by Scarponi et al. (2013) demonstrated that time averaging in the Po Plain fossil record varies predictably with sequence stratigraphic patterns. Specifically, time averaging gradually increased upward through the TST and was most extensive within the condensed sections (MFS). This trend was reserved in the HST, with increasingly thicker and less time-averaged beds observed upward.

In summary, a distinctive sequence stratigraphic architecture of the Po Plain is well understood in terms of facies architecture, patterns driven by base-level changes, vertical and lateral changes in

rates of depositional processes, and the scale of time averaging affecting paleontological samples.

Sampling Methods and Data Sets

A total of 16 cores were selected from the southeastern Po coastal plain (study area) to ensure adequate coverage of both the Holocene and the Late Pleistocene cycles (fig. 1*A*). These cores were drilled as part of a large, multidisciplinary effort focused on understanding in detail the subsurface stratal patterns of late Quaternary Po Plain deposits (i.e., the new Geologic Map of Italy project; http://www.apat.gov.it/) and evaluating the groundwater salinity dynamic in the coastal aquifer near Ravenna (Greggio et al. 2012). Core spacing (fig. 1*A*) varies as a function of paleocoastal morphology (Amorosi et al. 2003) and the large-scale patterns of the last marine ingressions (fig. 1). Hence, a large number of cores occur in the northernmost portion of the study area, where transgressions flooded wider areas due to the low gradient/inclination of the plain (fig. 1*A*). Southward, the marine deposits become progressively restricted by the Apennines (fig. 1*A*).

The sequence stratigraphic interpretation of these cored deposits has already been developed on the basis of integrated sedimentologic, geochemical, and micropaleontological evidence (Amorosi et al. 2003 and references therein). Various micropaleontological tools (foraminifers, ostracods, and pollen) have been employed to reconstruct the spatial and temporal development of depositional environments within Po coastal plain deposits, highlighting short-term environmental oscillations under strong glacio-eustatic control (Amorosi et al. 2004). In addition, 11 of the 16 cores have been time constrained using ^{14}C radiometric dates, mainly on the basis of peat layers and ^{14}C-calibrated amino acid racemization dates for ~250 bivalve shells (Scarponi et al. 2013 and references therein).

A total of 611 bulk samples (~375 cm^3 each) were collected from the studied cores with vertical spacing of 4 m or less. Samples were dried (24 h at 45°C), soaked in ~4% H_2O_2 (≤4 h, depending on lithology), and wet sieved down to 1-mm screens. For some samples (massive clay), this process was repeated at least two times. For each sample, all mollusk specimens (the most abundant macrofossil group represented in cores) were identified to the species level (when possible) and counted. Less frequent macrobenthic remains (such as serpulids or crustaceans) were noted but not counted. The term "specimen" is applied here to a complete fossil or a fragment that can be reliably identified as a unique individual (e.g., apex for gastropods or umbo for bivalves). In the case of bivalves, each valve or unique fragment was counted as 0.5 specimens. Along with species counts, the lithology, systems tract, lithofacies, core depth, site altitude, and age (Holocene or Pleistocene) were included for each sample on the basis of well-log information stored in the geological cartography database of the Regione Emilia-Romagna and from published (e.g., Amorosi et al. 1999, 2003) and unpublished (for cores 15–17) data.

The Po Plain Mollusk Data Set. The raw data set produced from cores included 131,780 specimens of bivalves, gastropods, and scaphopods. The data matrix contained 234 species representing 152 genera of mollusks. All analyses were conducted at the genus level (48% of the genera are represented by only one species) to suppress problems inherent to species-level interpretations, especially considering that taxonomic identification was done by multiple researchers. Supplementary multivariate ordination and bathymetric correlations were also conducted at the species level to assess if the species-level data yielded results consistent with those derived by genus-level analyses (see the supplementary material, available online).

In addition to LST deposits, proximal (up-dip) cores included a large portion of alluvial/continental samples. These samples are dominated by freshwater and terrestrial genera that likely respond to different environmental drivers with respect to the marine ones. Consequently, all analyses below are restricted to samples dominated by lagoon or marine genera. The removal of freshwater and terrestrial taxa (which account for <2% of specimens in the data set) did not reduce the number of samples and specimens in a substantial way, only the number of genera. In addition, to minimize analytical volatility and remove statistical outliers due to small sample size, all singletons (genera occurring in one sample only) and all small samples ($n < 20$ specimens after the removal of singletons) were excluded.

The criteria applied resulted in a minor loss of specimens and a substantial loss of exceedingly rare genera and inadequately small samples (fig. 2), especially from alluvial/continental depositional environments. Indeed, all LST (and a great part of FSST) samples were removed from the culled data set. The final data set used in all subsequent analyses includes 297 samples, 128,603 specimens, and 196 species grouped in 104 genera.

Independent Ecological Estimates of Preferred Species and Genus Depths. We obtained present-day water

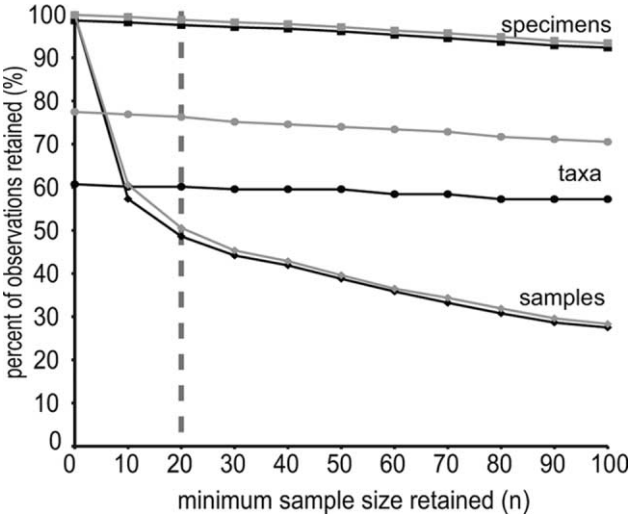

Figure 2. Effect of removal of small samples, singletons, and nonmarine taxa on the percentage of information retained. The loss of information for the Po Plain–culled data, with no singletons and no nonmarine taxa (black), is only slightly more pronounced than that observed for the raw data (gray) when considering specimens and samples. However, the removal of nonmarine taxa and singletons greatly reduces the data set at the taxon level, where there is a dramatic separation between the data sets (black and gray lines). All final analyses were based on the marine data set with samples that contained at least 20 specimens. The dashed line indicates the final data set.

depth estimates of extant genera from the New Technologies, Energy, and Environment Agency (ENEA) Italian mollusk census database (http://www.santateresa.enea.it/wwwste/malaco/home.htm; table 1). The ENEA census is part of a coordinated effort from multiple surveys that catalogued their collections of the Mediterranean mollusks and made them publicly available. The ENEA database includes information on such things as locality (latitude/longitude), collection methods (dredging, immersion, etc.), water depth (m), substrate (sandy, rocky, muddy, etc.), and the number of individuals collected (both live and dead). These data were used to acquire independent quantitative estimates of the preferred water depth for genera commonly found in the core material. Calculated water depths for individual species for each genus were based on samples from the ENEA data set that had three or more live specimens in the collection, suggesting that their presence in the sampled location was not due to transport. The counts for both live and dead specimens were combined for each collection that met this criterion, and the total numbers of individuals from all the available samples with their respective collected depths were recorded.

Hence, for each species retrieved in the Po coastal plain deposits, its preferred bathymetry was estimated (via the ENEA database) as the specimen-weighted average depth. The genus-level water depth (ENEA genera [EG]) was then calculated by averaging species-level estimates. Thus, for genera represented by only one species, species depth and EG are equivalent. We obtained EG estimates for 24 genera (represented by 44 species) that were most common in the core material (table 1).

Analytical Methods

The final Po Plain data set (see above) represents a large, multivariate data matrix suitable for the development of quantitative environmental estimates applicable to core samples included in the data set. This data set is available on request from the first author. On the basis of initial analyses of three cores (Scarponi and Kowalewski 2004), we postulate that bathymetry is the primary correlative of variation in faunal composition across the sampled cores. Here, we employ a series of multivariate strategies to evaluate this hypothesis using a large data set derived from a three-dimensional network of core samples. In addition, this hypothesis is further tested by means of ecological estimates of preferred species and genus depths derived independently using present-day bathymetric data (see the description of the ENEA data set above).

Multiple strategies can be employed to develop a bathymetric model suitable for interpreting different tracts of facies in a sequence stratigraphic perspective. Here, we focus on two analytical techniques: weighted averaging and a posteriori ordination.

Weighted Averaging. Weighted averaging, a precursor to correspondence analysis (CA), is a direct, one-dimensional ordination strategy (Hill 1973; McCune and Grace 2002) where external environmental information is used to ordinate samples or taxa. In this particular case, genus-preferred bathymetry attributes are employed to develop sample-level paleoenvironmental (water depth) estimates. Here, the average water depth of a Po Plain sample is computed by considering all genera present in that sample for which EG estimates (=genus-preferred depths via relevant species-level estimates from the ENEA data set) are available (table 2; fig. 3). The estimated sample depth via weighted averaging (S-WA) is computed as the mean EG of the abovementioned genera weighted by the number of speci-

Table 1. Summary of the Selected 24 Genera from the Po Plain and the New Technologies, Energy, and Environment Agency (ENEA) Data Sets

	Po Plain			ENEA			
Genus	Rank	No. individuals in fossil samples	No. species	EG (m)	No. specimens	No. samples (collections)	SD (m)
Lentidium	1	84,373	1	−2.86	18,590	20	1.90
Heleobia	2	10,542	1	−.95	5921	3	.28
Varicorbula	3	6027	1	−13.51	40,527	121	6.56
Chamelea	4	5363	1	−7.71	17,590	57	4.10
Abra	5	3120	5	−7.14	5491	65	6.88
Spisula	6	2398	1	−6.60	3739	48	7.31
Turritella	7	2355	1	−18.26	3199	31	23.92
Tellina	8	1903	3	−11.66	1684	85	8.92
Donax	9	1683	3	−1.36	4510	31	3.90
Bittium	10	1424	2	−4.91	4169	30	3.33
Cerastoderma	11	1037	1	−.326	5593	18	.96
Nassarius	12	902	4	−6.99	1334	50	5.93
Dosinia	13	710	1	−5.58	729	29	3.39
Antalis	14	647	3	−19.24	421	27	11.01
Bela	16	458	3	−6.93	46	5	10.20
Nucula	17	388	1	−19.37	1617	85	12.47
Kurtiella	18	364	1	−13.14	12,981	41	6.54
Glycymeris	19	326	2	−7.67	266	11	6.78
Pitar	22	251	1	−16.68	199	14	7.49
Acanthocardia	23	242	4	−9.54	807	29	10.70
Euspira	24	239	2	−19.24	229	22	20.59
Acteon	27	149	1	−8.00	52	8	16.01
Fustiaria	28	137	1	−15.76	33	3	3.90
Mimachlamys	36	66	1	−14.89	564	20	12.89

Note. Rank abundance, number of individuals, and number of species are from the fossil Po Plain data set, and estimated mean water depths (EG), standard deviations, and sample information are from the ENEA data set.

mens per genus. For example, if a sample contains four genera with EG estimates, the sample depth is estimated using EG values of the four taxa (e.g., −5.58, −0.33, −2.86, and −13.16 m) weighted by the number of specimens of those genera present in that core sample (e.g., 150, 10, 28, and 56). In this example, the resulting sample depth (S-WA) expressed in meters would be −6.79 m. The advantages of this strategy are its analytical simplicity and derivation of a univariate ordination function that is a linear combination of variables (taxa) expressed in environmentally meaningful units. In the case of our data, the obvious drawback of the approach is the partial use of specimen counts describing a given sample (i.e., if a sample is dominated by genera for which EG estimates are not available, the sample depth estimates can be unreliable). Although the EG estimates are available for the most common genera, some samples are affected by this problem here, and their position along the ordination axes may be inaccurate (only one sample did not contain any genus with EG estimates). Weighted averaging also allows for a reciprocal derivation of genus scores from S-WA scores. The preferred genus depth (G-WA) is then computed as a specimen-weighted average of S-WA scores of all samples from which the targeted genus has been retrieved (see table 2). This approach is somewhat circular because S-WA values were derived from EG estimates. However, this redundancy allows for testing the robustness of sample depth estimates and for estimating G-WA depth estimates for all genera in the data set (even if it should be reliable only for genera that nowadays peak in the range of depositional environments recorded by studied Po coastal plain deposits). Note that for the 24 genera with modern depth information, G-WA and EG values should correlate highly—a low correlation would indicate that the 24 genera are insufficient to generate robust depth estimates and/or that the range of depositional environments recorded in the Po Plain data sets does not strongly overlap with those recorded by the ENEA marine data set (i.e., the ENEA data set is not representative of the Po Plain data set). Finally, we note here that this approach is analytically related to but not synonymous with CA, an indirect ordination approach that can be computed by iterative reciprocal averaging of samples and taxa starting from arbitrary score configurations (Gauch 1982). The fundamental difference is that the weighted averaging, as employed here, is based on external

Table 2. Different Types of Depth Estimates of Samples and Genera Used to Develop Bathymetric Models for the Po Plain Data Set

Depth estimator	Data sets used	Derivation	Scope	Comments	Equation[a]
EG: preferred genus depth	ENEA	Weighted averaging of species-level data	24 genera	Direct estimates from ecological surveys	$\mathrm{EG} = \frac{\sum_{i=1}^{n}(D_i \cdot \mathrm{SP_s})}{N_s}$
S-WA: sample depth by weighted averaging	Po Plain, ENEA	Weighted averaging of EG estimates	All samples	Weighted averaging of samples	$\text{S-WA} = \frac{\sum_{i=1}^{n}(\mathrm{EG}_i \cdot G_s)}{N_{EG}}$
G-WA: preferred genus depth by weighted averaging	Po Plain, ENEA	Weighted averaging of S-WA estimates	All genera	Reciprocal estimates by weighted averaging of sample depth (S-WA)	$\text{G-WA} = \frac{\sum_{i=1}^{n}(S - \mathrm{WA}_i \cdot G_s)}{N_g}$
S-DC: sample depth by posteriori calibration	Po Plain, ENEA	DCA	All samples	Posteriori calibration of DC1 scores using S-WA estimates	$\text{S-DC} = (-0.0351 \cdot \mathrm{DC_s}) - 1.5575$
EG-DC: preferred genus depth by posteriori calibration	ENEA	DCA	24 genera	Posteriori calibration of DC1 scores using EG depth estimates	$\text{EG-DC} = (-0.0479 \cdot \mathrm{DC_g}) + 1.2479$
G-DC: preferred genus depths by posteriori calibration	Po Plain, ENEA	DCA	All genera	Posteriori calibration of DC1 scores using G-WA estimates	$\text{G-DC} = (-0.0493 \cdot \mathrm{DC_g}) + 1.9042$

Note. D = depth of selected species within a sample; $\mathrm{DC_g}$ = DC1 ordination scores for genera; $\mathrm{DC_s}$ = DC1 ordination scores for samples; DCA = detrended correspondence analysis; ENEA = New Technologies, Energy, and Environment Agency; G_s = number of specimens of a given genus within a sample; N_s = total number of specimens for the given species in the entire ENEA data set; N_{EG} = total number of specimens in a sample with EG depths from the Po Plain data set; N_g = total number of specimens for a selected genus in the entire Po Plain data set; $\mathrm{SP_s}$ = number of specimens of a given species within a sample.
[a] After filtering samples with less than three live specimens of a given genus (see "Sampling Methods and Data Sets").

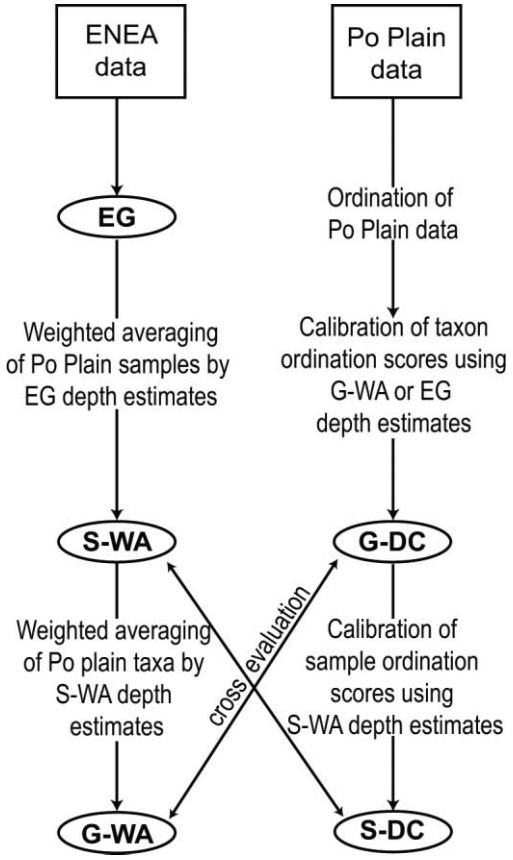

Figure 3. Flowchart illustrating the process of estimating water depth using multiple approaches based on the ecological (New Technologies, Energy, and Environment Agency [ENEA]) and Po Plain data sets. Squared segments indicate data matrices, and circled segments indicate calculable depth estimates. See table 2 for explanations of acronyms.

environmental scores (preferred genus water depth, in this case), whereas CA represents an unconstrained (indirect) approach where ordination is obtained from sample versus taxa similarities without a priori constraints given by external variables.

Indirect Ordination Approaches. Initially, three indirect (unconstrained) ordination procedures often used with compositional data (e.g., Holland et al. 2001; Miller et al. 2001; Olszewski and Patzkowsky 2001; Kowalewski et al. 2002; Holland 2005; Zuschin et al. 2006; Holland and Patzkowsky 2007; Ivany et al. 2009; Zuschin et al. 2011; Ayoub-Hannaa et al. 2013; Hendy 2013; Zuschin et al. 2014) were applied to the relative abundance matrix: CA, detrended CA (DCA), and nonparametric multidimensional scaling (NMDS) using the Bray-Curtis dissimilarity measure. All three methods produced comparable ordinations and strong post hoc correlations with independent EG estimates of genus-preferred depth. We report here the results from DCA only. Although DCA suffers from multiple drawbacks (Beals 1984; Kenkel and Orlóci 1986; Minchin 1987; Wartenberg et al. 1987; Jackson and Somers 1991; McCune and Grace 2002), it is often effective in reducing an arch effect (Hill and Gauch 1980), especially when the distribution of taxa is overwhelmingly controlled by a single gradient, which is likely the case here (Scarponi and Kowalewski 2004), as also indicated by a strong arch effect observed in the CA ordinations of the Po Plain data set (see below). This method has been used successfully in numerous studies comparing stratigraphic and paleoecological data (see references in Patzkowsky and Holland 2012). Like DCA, the NMDS ordinations displayed a reduced arch effect, whereas CA produced ordinations with a strong arch effect that was evident in both the genus and the sample ordinations.

The software package PAST (Paleontological Statistics; ver. 2.07; Hammer et al. 2001) was used to obtain DCA scores using default settings with detrending on and 26 segments selected, the number of first-axis segments that are rescaled to counteract the arch effect. Relative abundance values were log transformed using the downweight option to minimize distortion of very abundant genera (Hammer et al. 2001). SAS and SAS/IML software was used to create the relative abundance data matrix and to perform supplementary tests (SAS Institute 2002). Bathymetric calibrations were calculated using ordinary least squares of DC1 scores against several types of depth estimates for sample and genera derived from the EG values for the 24 common genera in the Po Plain data set (table 2). For sample depth, depth-calibrated scores (S-DC) can be derived by regressing DC1 scores against S-WA estimates obtained by weighted averaging (see above). For genera, depth-calibrated scores (EG-DC) can be similarly derived using original EG estimates obtained from ENEA. Alternatively, genus depth estimates (G-DC) can be derived using G-WA scores. The depth-calibrated indirect ordination can then be cross evaluated against direct ordination estimates derived by weighted averaging, as discussed above (fig. 3).

Cross Correlations of Bathymetric Models. The use of multiple strategies allows us to derive partly redundant estimates of sample depth (S-WA vs. S-DC) and genus depth (G-WA vs. G-DC). The latter can be also contrasted against EG depth estimates derived from the ENEA database either directly (EG) or indirectly (EG-DC). This redundancy allows for multiple cross assessments of the consistency of bathymetric estimates derived using

different analytical strategies and for assessing relative biases across bathymetric models (table 2). Ideally, water depths calculated via weighted averaging (S-WA) should correlate tightly with DC1-calibrated water depths (S-DC) and yield quantitatively consistent depth estimates. Similarly, the two genus-level calibrations (EG-DC and G-DC) should result in equivalent DC1-calibrated depth estimates congruent with direct ecological estimates from modern genera (G-WA). For sample and genus-level estimates, high pairwise correlations and similar absolute depth estimates are desired across all the models.

Results

Weighted Averaging. Genus depth (EG) estimates from the ENEA and the Po Plain data set (G-WA) predict comparable water depth ($r^2 = 0.96$, $n = 24$, $P < 0.0001$; fig. 4). The G-WA parameter slightly underestimates water depth relative to the EG parameter. However, this offset is relatively minor (<1 m), indicating that the two metrics provide a reasonably consistent estimate of the preferred genus depth. In figure 4, the few more notable departures (these can exceed 1 m but are all below 5 m) of individual genera from the EG versus G-WA regression line are observed. These can be explained as the result of differences in species representing those genera in the ENEA versus Po Plain data sets. For example, the preferred depth of the genus *Abra* on the basis of its abundance in Po Plain samples is G-WA = −2.8 m, whereas the ENEA-based estimate is EG = −7.1 m. This relatively high offset reflects the different proportional weight of *A. segmentum*, a brackish species that is rare in the ENEA marine data set (only six occurrences among 135 used in the computation) but abundant in the Po Plain data set (1138 occurrences among 3120).

Water depth estimates of Pleistocene and Holocene samples based on direct ordination display a left-skewed distribution, with shallow-water samples ~0 to −4 m dominating the data set (fig. 5). The Pleistocene sub–data set has a limited number of samples ($n = 44$), producing a less pronounced left-skewed depth pattern than the Holocene. Depth distributions grouped by sequence stratigraphic position reflect the generalized water depth for each depositional sequence (fig. 6). FSST samples include primarily shallow-water sites, and maximum flooding samples span a relative wide range of depths (−2 to −16 m). TST samples array across the depth gradient with a greater number of samples occurring around endpoints at −15 and −3 m in depth, suggesting a possible bimodal distribution. The bimodal distribution can be a result of variable sampling intensity of cores across the study area and potential differential preservation within the network of cores. The left-skewed distribution of the HST samples can be explained by shallow-water samples (~0 to −4 m) dominating the data set because the HST here is generally represented by fast stacking of thick sand bodies subject to low compaction, resulting in an overrepresentation of shallow-water sites in the data (see also Holland and Christie 2013; Scarponi et al. 2013).

Indirect Gradient Analysis. DCA ordination of mollusk genera from the Po Plain data set revealed a wedge-shaped distribution of taxa, with an in-

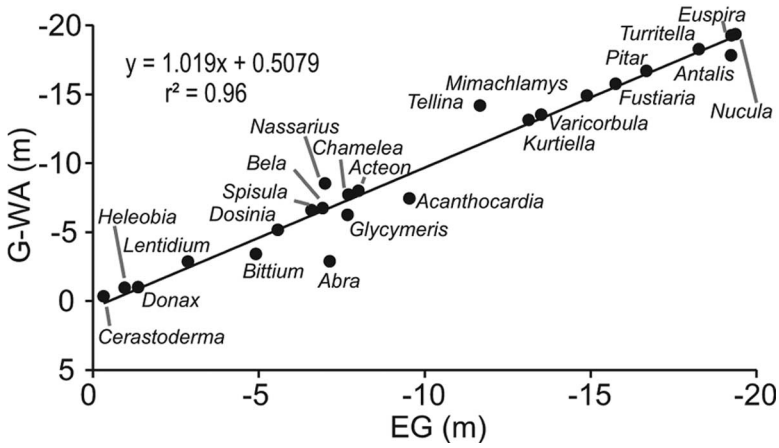

Figure 4. Bivariate plot of the weighted-average water depth estimates for 24 genera using preferred water depths from the New Technologies, Energy, and Environment Agency website (EG) and the Po Plain data set (G-WA). An ordinary least squares model (black line on the plot and numbers in the upper left corner) indicates that G-WA is an excellent predictor of EG.

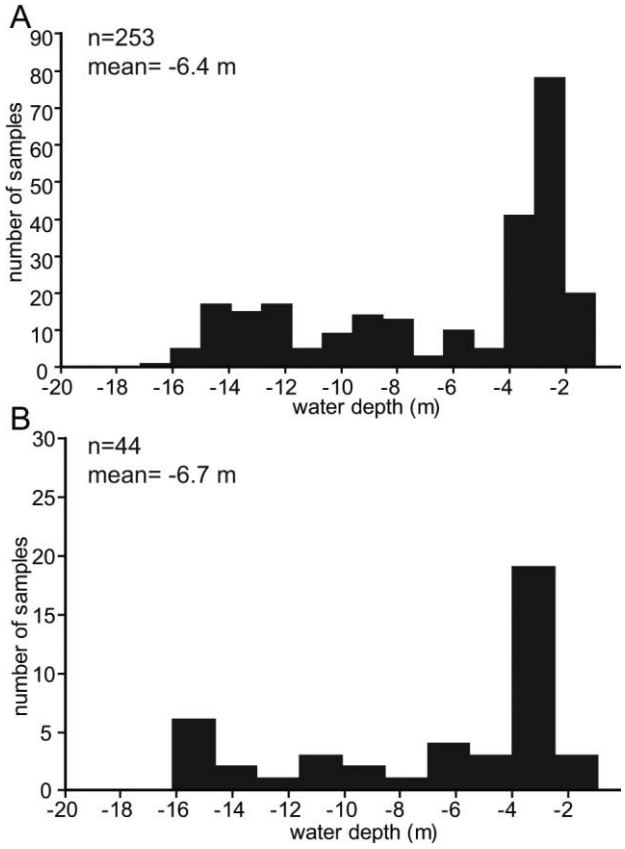

Figure 5. Distribution of sample water depths (S-WA). *A*, Holocene. *B*, Pleistocene.

creasing range of DC2 scores toward low DC1 score values (fig. 7). The wedge-shaped pattern may be due to distortions related to detrending (as seen in Bush and Brame 2010), but it may also capture additional environmental information, as appears to be the case for Po Plain mollusk associations (Scarponi and Kowalewski 2004). For the lowest DC1 scores (0–120), the DC2 scores of genera vary widely (from −176 to 695). As DC1 scores increase, the variation along the DC2 axis gradually decreases (fig. 7). The distribution of the 24 common extant genera (table 1) along DC1 suggest that genera are ordinated by water depth, with the shallowest-water taxa (e.g., *Heleobia*, *Lentidium*, and *Donax*) having lower DC1 scores and increasingly deeper-water taxa (e.g., *Turritella*, *Euspira*, and *Antalis*) having higher DC1 scores. To evaluate this relationship, the DC1 scores were evaluated against the two depth proxies (ENEA [EG] and Po Plain [G-WA]) using ordinary least squares (fig. 7, *insets*). For both genus depth estimators, the DC1 scores are a robust linear predictor of depth, indicating that the primary gradient observed in the ordination of genera is water depth (and/or its environmental correlatives). For the ENEA water depth estimate, DC1 is a linear predictor with a model error (root mean square error) of 2.6 m ($r^2 = 0.82$, $n = 24$, $P < 0.0001$; fig. 7, *inset A*). For the G-WA depth estimate, the DC1 scores perform comparably well ($r^2 = 0.81$, $n = 24$, $P < 0.0001$; fig. 7, *inset B*), with a model error of 2.8 m. DCA ordinations at the species-level displayed a weaker association between DC1 scores and the EG water depth estimates ($r^2 = 0.41$; see the supplementary material).

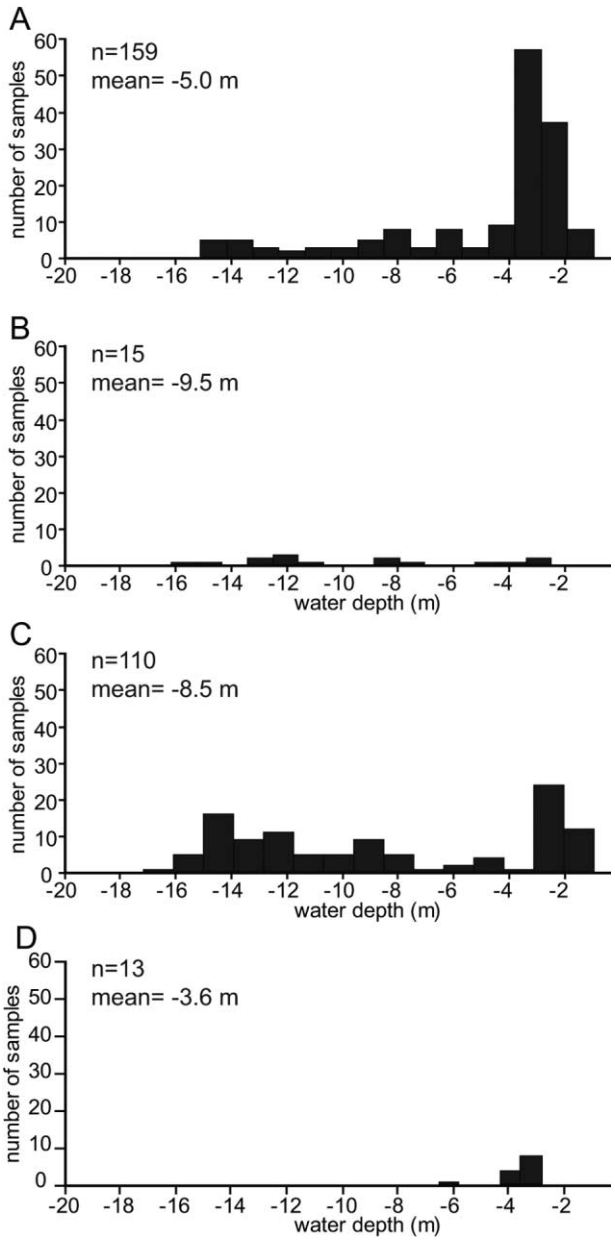

Figure 6. Distribution of sample water depths (S-WA) grouped by highstand systems tract (*A*), maximum flooding zone (*B*), transgressive systems tract (*C*), and falling stage systems tract (*D*).

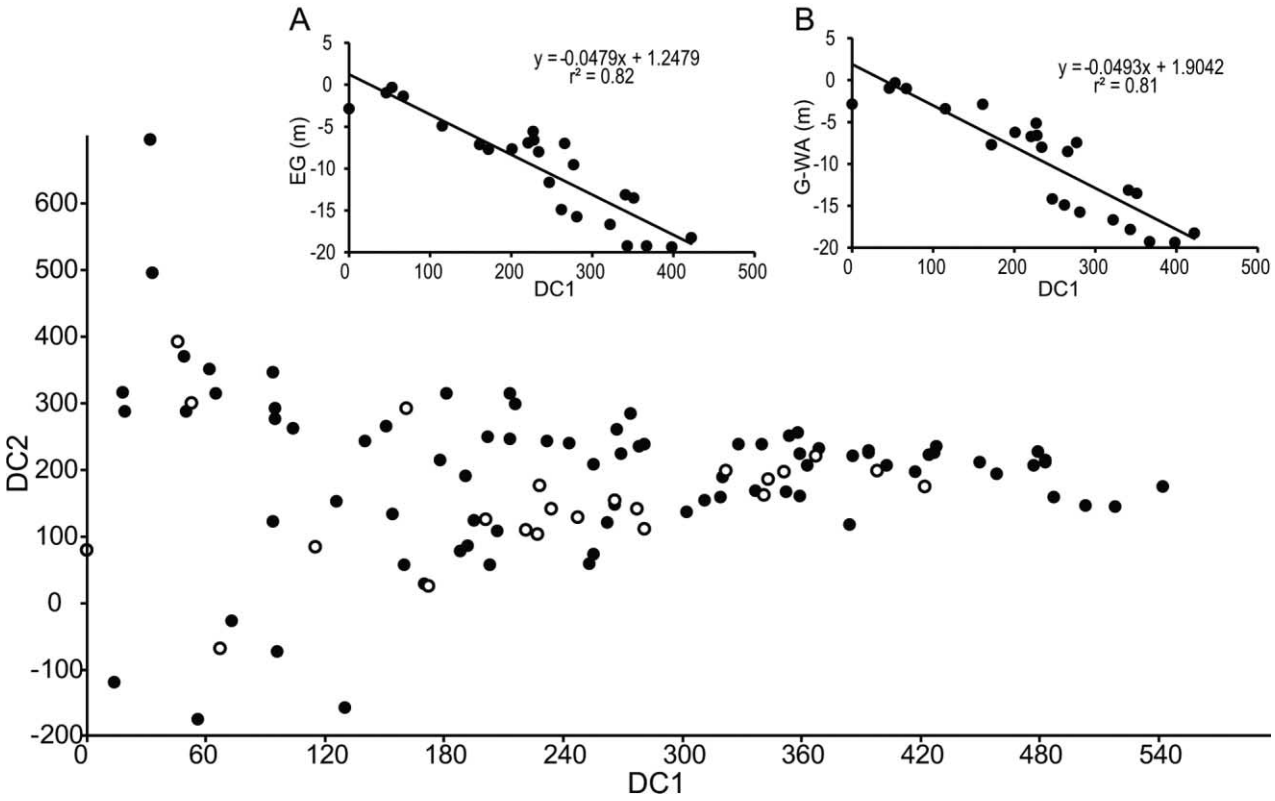

Figure 7. Detrended correspondence analysis (DCA) of genera (black circles) with the 24 genera used for bathymetric analysis (white circles). Deeper-water genera have high DC1 scores and comparable DC2 scores, and brackish/shallow-water genera have low DC1 scores and variable DC2 scores. Eigenvalues: for DC1, 0.76; for DC2, 0.44. Percent variance: for DC1, 57.7%; for DC2, 19.6%. It should be noted, however, that the percentage of explained variance of DCA axes is suspect due to detrending and rescaling (Patzkowsky and Holland 2012). *Insets*, ordinary least squares (OLS) regression for DC1 scores and EG depth estimates based on New Technologies, Energy, and Environment Agency data (*A*) and OLS for DC1 scores and G-WA depth estimates derived from paleontological data using weighted averaging (*B*).

When samples are plotted in the same coordinate system that was used above for genera (fig. 7), they also form a wedge-shaped ordination pattern, although samples with low DC1 scores are decidedly bimodal in terms of their DC2 scores, forming two distinct sample clusters (fig. 8). Depth estimates of the ordinated samples derived by weighted averaging of the ecological data (S-WA) range from ~0 to ~18 m. Compared with the genus-level analyses given above, deeper-water samples have high DC1 scores and shallower-water samples have low DC1 scores. Samples with low DC1 scores (<140) and high DC2 scores (>250) represent brackish/shallow-water environments, such as lagoonal and back-barrier deposits. Samples with both low DC1 scores and low DC2 scores (<250) represent outer lagoon to shallow marine samples, suggesting that variation along the DC2 axis may represent salinity and energy (as suggested by Scarponi and Kowalewski 2004). DC1 scores also appear to be a good predictor of sample water depth estimates (S-WA) derived by direct ordination via weighted averaging of EG ($r^2 = 0.92$, $n = 264$, $P < 0.0001$; fig. 8, *inset*). Sample DC1 scores produce depth estimates to the nearest 1.3 m (fig. 8, *inset*). Samples with estimated depths deeper than −5 m display a tight linear correlation, but residuals for samples with low DC1 scores (shallower than −5 m) are more variable. Overall, S-WA depths correlate tightly with DC1 scores.

A majority of the studied cores yield samples that vary substantially in DC1 scores, reflecting both shallowing and deepening trends through time (fig. 9*A*). Proximal cores generally represent shallower settings and do not capture deeper environments present in more distal cores. When the ordination of samples is coded by age, both the Pleistocene and the Holocene samples cover the entire depth gradient along axis 1 (fig. 9*B*). In assessment of sequence stratigraphic patterns, both

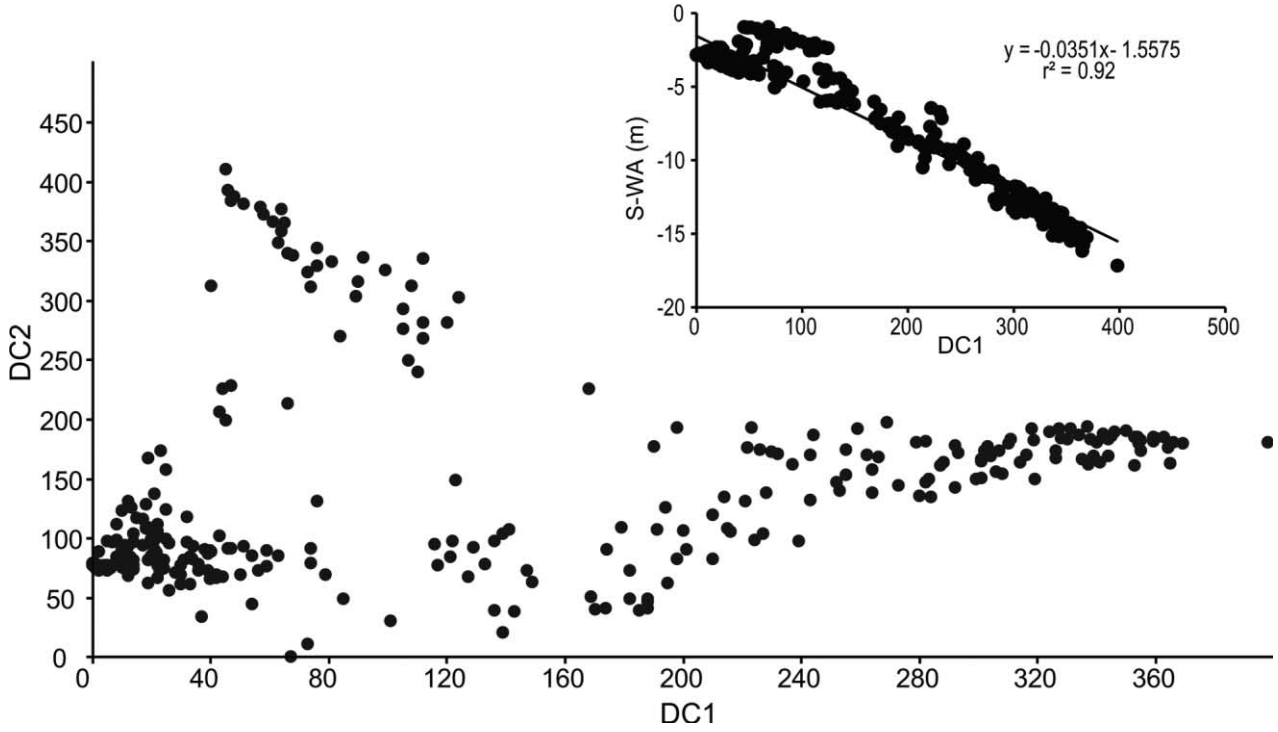

Figure 8. Detrended correspondence analysis of samples (n = 297). *Inset*, scatterplot of sample water depth estimates graphed against sample DC1 scores (n = 297). Root mean square error = 1.27 m.

TST and HST samples spread across DC1 and occur in both DC2 clusters (fig. 9*C*). Samples identified as MFS/maximum flooding zone (MFZ) spread across DC1 and have intermediate DC2 scores for both landward and seaward cores (fig. 9*C*). FSST samples have low DC1 scores because they represent nearshore environments, limiting the extent of FSST samples along the depth gradient (fig. 9*C*). There is no distinct separation of HST and TST samples (via MFZ) along DC1 because cores range across the depositional profile, mixing TST and HST samples from sites with different proximity to the regional depocenter.

Cross Evaluation of Calibrated Bathymetric Models. Water depth estimates of genera derived by a direct EG-constrained approach (G-WA) show a high correlation with those obtained by the unconstrained and calibrated approach (i.e., G-DC), thus indicating that the two approaches estimate water depth for the selected 24 taxa in a concordant manner (fig. 10*A*). The calibrated DC1 sample depths (S-DC) are comparable to the weighted-average sample depths (S-WA), indicating that the analyses are also consistent for sample estimates (fig. 10*B*; table 3).

Although the different metrics used here correlate tightly, they produce somewhat different absolute depth values for genera and samples (i.e., they are somewhat offset relative to each other, with genus depth estimates more widespread than sample depths for DC1; fig. 10). This is understandable as samples are a combination of genera; hence, bathymetry estimates of samples will tend to show a restricted range depth unless samples at both ends record only the shallowest/deepest genus.

Depth calibrations of sample-level S-DC and genus-level EG-DC (or G-DC; fig. 11*B*; i.e., the approach developed in Scarponi and Kowalewski 2004) were compared using intervals of 100 for the DC1 scores (fig. 11). Similar results are produced with both models, with S-DC slightly overestimating depths relative to the other approach (fig. 11). With shallow DC1 scores (DC1 = 100), EG-DC (or G-DC) and S-DC calibrations produced depths with a difference smaller than 1.6 m: −3.5 (3.0) and −5.1 m, respectively (fig. 11). With higher DC1 scores (DC1 = 400), the difference between the two metrics was slightly more pronounced, with the two calibrations being within 2.3 m of each other: −17.9 (−17.8) and 15.6 m, respectively (fig. 11). Hence, with DC1 scores ranging from 0 to 400, EG-DC and G-DC depth estimates produce a wider depth gradient (for EG-DC, from +1.2 to −17.9 m; for G-DC, from +1.9 to −17.8 m) than S-DC depth estimates (−1.6 to −15.6 m).

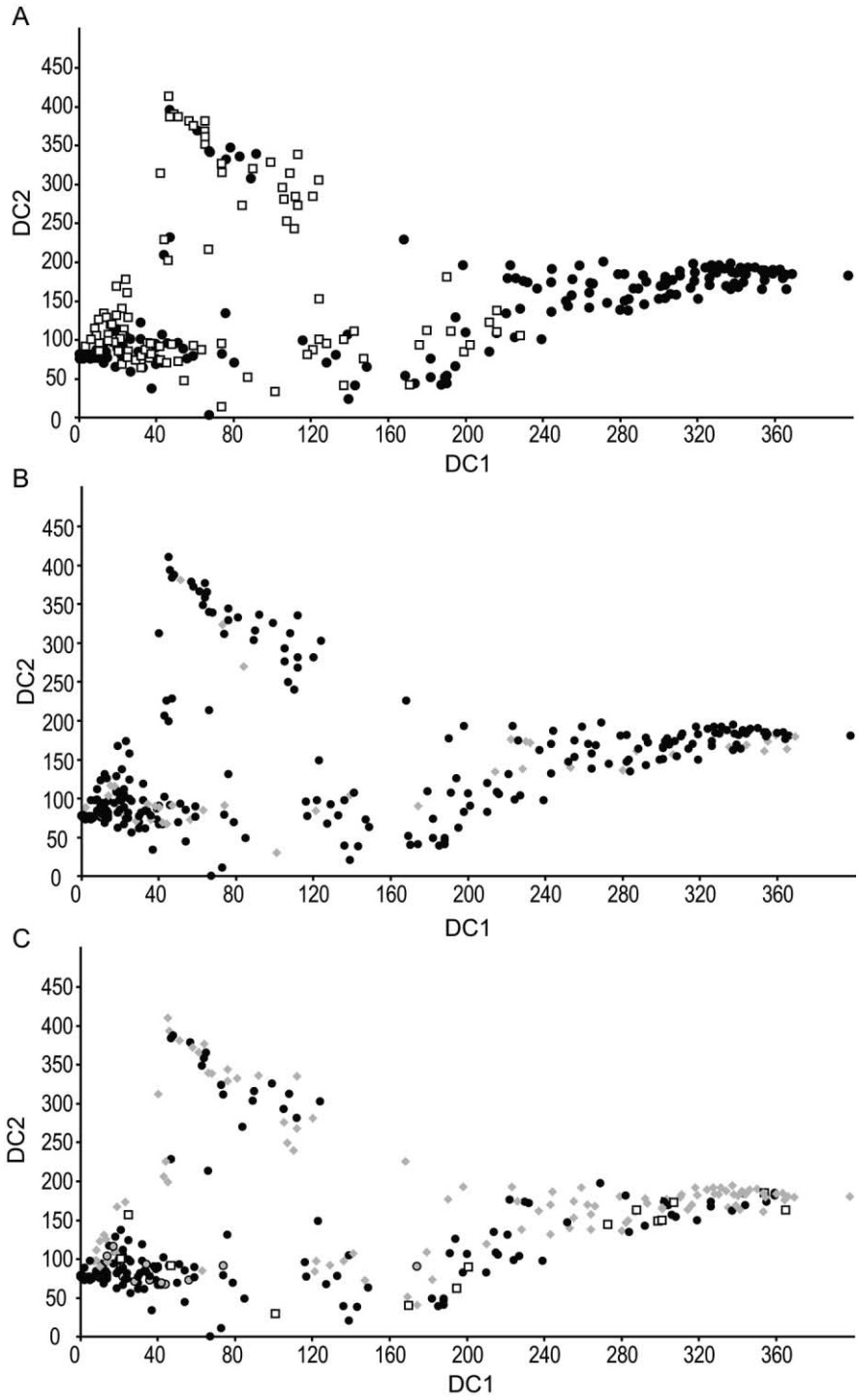

Figure 9. Detrended correspondence analysis of samples ($n = 297$). *A*, Position along depositional profile. Proximal cores are indicated by white squares (cores 8, 13–15, 18–20), and distal cores are indicated by black circles (cores 1–7, 16, 17). *B*, Age. Gray diamonds indicate the Pleistocene, and black circles indicate the Holocene. *C*, Sequence-stratigraphic position. Black-outlined gray circles indicate falling-stage systems tract samples, gray diamonds indicate transgressive systems tract samples, open squares indicate maximum flooding zone samples, and black circles indicate highstand systems tract samples.

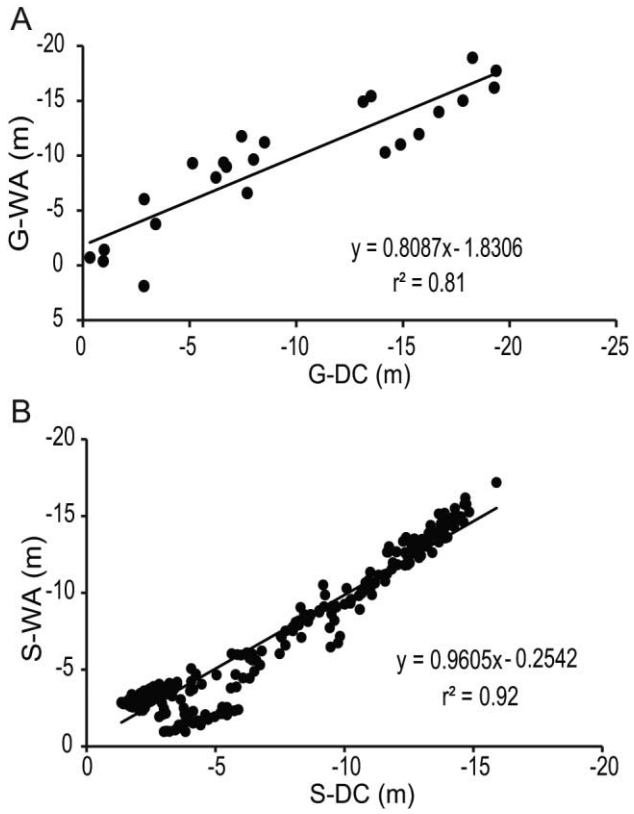

Figure 10. Scatterplot of estimated and calibrated water depths. *A*, Comparison of genus-level estimated water depths with detrended correspondence analysis (DCA)–calibrated genus water depths of the 24 taxa. *B*, Comparison of S-WA-estimated water depths with DCA-calibrated S-DC.

Bathymetric Models and Their Application to Sequence Stratigraphy. S-WA and S-DC depth estimates (see the equations in table 2) were calculated for each sample, and the resultant water depth estimates were plotted stratigraphically (fig. 12). Both parameters showed similar depth trends displaying gradual deepening-upward followed by shallowing-upward depth signals. S-WA and S-DC are slightly offset compared with each other in both Pleistocene and Holocene cores, with S-DC estimating slightly deeper depths than S-WA except in core 3 from the Late Pleistocene, where S-WA estimates deeper depths during maximum flooding (fig. 12*B*). The stratigraphic plots of bathymetrically related trends delineate and match the independent and expected sequence stratigraphic interpretations available for the Pleistocene and Holocene succession of the Po Plain (fig. 1). Unlike core 3, however, cores from proximal settings are generally less easy to interpret, either showing substantial stratigraphic disagreements with sequence stratigraphic interpretations (fig. 12*C*) or revealing more complicated patterns than those suggested by the regional sequence stratigraphic model (fig. 12*D*).

Water depths based on S-DC estimates of independently derived MFS plotted by core (fig. 13) show slight offsets in maximum water depths relative to each other across the Po Plain deposits. Southern cores range in maximum water depths from 7 to 12 m (fig. 13*B*) followed by a deeper-water signal in northern cores, with maximum water depths of 12 to 16 m at peak transgression (fig. 13*A*).

Discussion

The water depth estimates derived from genus- and sample-based bathymetric models are mutually consistent and generally agree with the sequence stratigraphic interpretations of the Po coastal plain (with a few exceptions in very proximal areas). However, their utility may be more limited when applied to sedimentary basins in which fossil samples are dominated by either extinct genera or extant genera with poorly understood ecology and bathymetric distribution. The approaches worked well here because late Quaternary mollusk assemblages preserved in Po Plain deposits have remained remarkably unchanged over the present and last interglacial (Scarponi and Kowalewski 2007). Nevertheless, the results affirm the general notion that in marine systems bathymetry and depth-related variables can represent an overriding control on species composition. This indicates that indirect ordination approaches may provide a successful indirect proxy of depth (without absolute depth calibration) when also applied to older sedimentary basins (e.g., Holland et al. 2001; Hendy 2013).

An additional limitation, specific to the direct ordination approach, is its limited reliability for

Table 3. Correlation Coefficients of Depth Estimates

Depth estimate	*n*	Pearson's *r*	r^2	95% CI	*P* (α = .05)
G-WA vs. G-DC	24	.90	.81	.69–.93	.0001
S-WA vs. S-DC	264	.96	.92	.90–.94	.0001
G-DC vs. EG-DC	24	1	1	.99–1.00	.0001
G-DC vs. S-DC	5	1	1	.99–1.00	.0175

Note. See table 2 for explanations of acronyms. CA = confidence interval.

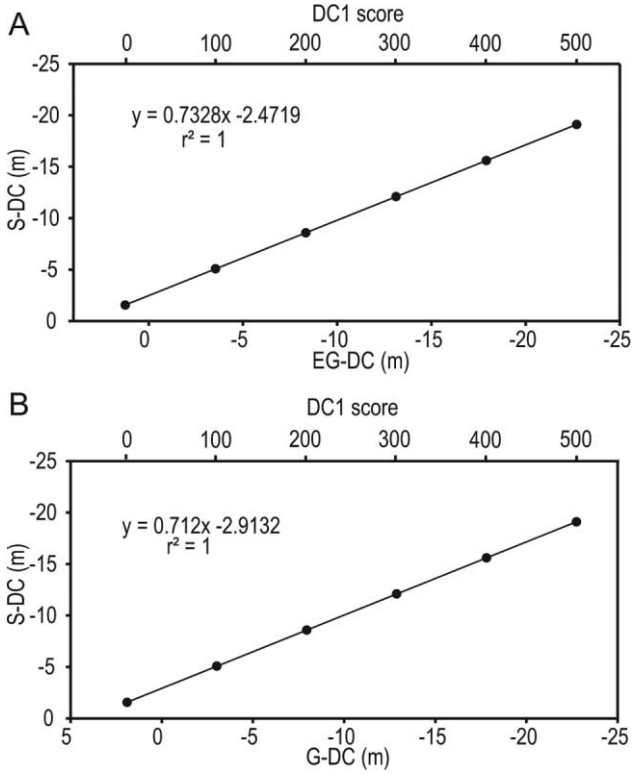

Figure 11. Bivariate plot of DC1-calibrated depths. *A*, Comparison of S-DC and EG-DC depth estimates for DC1 scores. *B*, Comparison of S-DC and G-DC depth estimates for DC1 scores.

samples dominated by genera for which EG estimates are not available. In the case of our data, only one sample in the culled marine data set did not contain any of the 24 taxa with EG water depth estimates, and it was not used in any of the analyses. Six of the 297 samples included only one genus of the 24 genera along with other minor taxa, but these samples represented primarily very proximal cores (back-barrier and estuarine facies). For samples affected by this problem, their position along the ordination depth axis may be substantially inaccurate. In this case or in case studies where the lack of ecological data at taxa level could hamper paleoenvironmental reconstructions, a correlation analysis between indirect and direct derived ordination estimates (fig. 11) can improve the paleoenvironmental accuracy of poorly defined samples and/or genera. The 24 extant genera used here provide a good representation of the entire bathymetric range, with their preferred depths spread relatively evenly from 0 to 20 m (fig. 4). The genus-level bathymetric estimates of the Po Plain genera are not synonymous with the bathymetric estimates of those in the Mediterranean today. This is because the computation of the preferred depth is based only on those species listed in the ENEA database that were recovered from the Po Plain sediments. The ENEA database includes additional species from those genera that occur in deeper-water settings that have not been sampled by the network of core samples used here. Moreover, even though some of those genera are represented by multiple species in the study area, they tend to have relatively narrow bathymetric distributions (median standard deviation of 6.8 m), and only a few genera occur over a substantial depth range (table 1). The results also highlight limitations of the proposed approach to identify bathymetric gradients. Ordinations of landward cores show mixed paleoenvironmental trends likely resulting from the influence of environmental variables that do not correlate strongly with bathymetry, such as variation in salinity or water energy across shallow-water settings. Coastal/back-barrier habitats that vary notably in salinity and water energy are thus particularly problematic to use for bathymetric reconstructions. The nonbathymetric sources of variations are particularly noticeable in figure 8, where samples with comparable DC1 scores separate into clusters along DC2, suggesting different salinity and energy regimes. This DC2 interpretation is consistent with microfaunistic and sedimentary inferences independently obtained for the same units (Amorosi et al. 1999, 2003).

The spatiotemporal scale of analysis may also limit the importance of bathymetric gradients. Redman et al. (2007; see also Grill and Zuschin 2001) found that at small spatiotemporal scales water depth becomes less relevant for controlling ordination gradients. Instead, life mode appears to be more appropriate for controlling variation from site to site, based on microhabitat change. These local heterogeneities may have also contributed to variability across landward cores observed in the bathymetric analyses of the Po Plain samples.

Another important caveat to the proposed approach is the confounding role of pooling data obtained along the regional depositional profile. Pooling of data from proximal and distal cores can mask stratigraphic signals that are discernible in two-dimensional cross sections parallel or perpendicular to the depositional profile of the basin. For example, Scarponi and Kowalewski (2004), using an array of three cores that did not differ dramatically in their location relative to the regional depocenter of the Po Basin, were able to recognize a distinct stratigraphic signal overprinting the ordination patterns, with TST, HST, and MFZ samples behaving

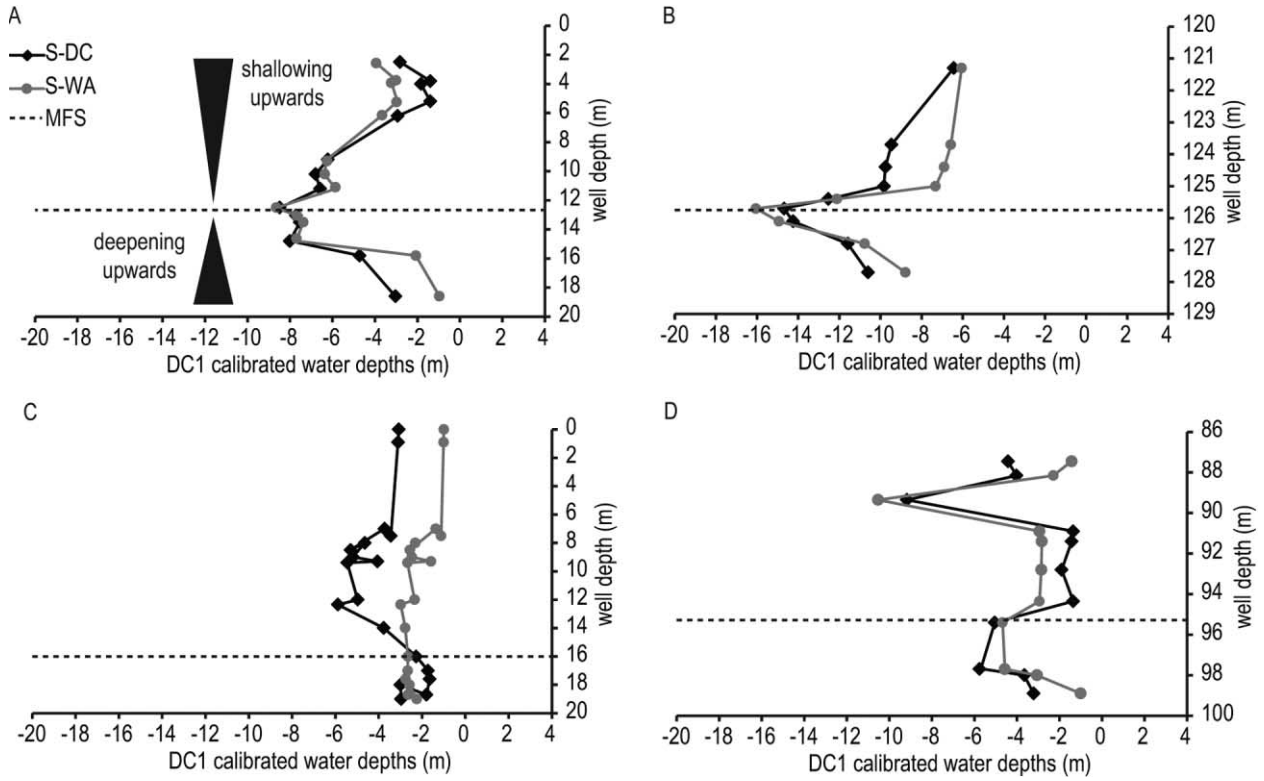

Figure 12. Stratigraphic patterns in DC1-calibrated water depths based on sample- and genus-level estimators. Maximum flooding shown is based on independent sequence stratigraphic interpretations (e.g., Amorosi et al. 2003, 2004). *A*, *B*, Examples of distal cores: Holocene transgressive-regressive cycle of core 3 (*A*) and Pleistocene transgressive-regressive cycle of core 3 (*B*). *C*, *D*, Examples of proximal cores: Holocene transgressive-regressive cycle of core 8 (*C*) and Pleistocene transgressive-regressive cycle of core 13 (*D*). MFS = maximum flooding surface.

in a predictable manner. However, when the ordination is based on a three-dimensional network of cores encompassing both distal and proximal settings, the sequence stratigraphic signals become obscured (fig. 9*C*). The indistinct pattern arising when samples are grouped by systems tracts is caused by pooling sites along the depositional profile, where proximal MFZ samples plot together with late HST samples from more distal samples. Moreover, deepening and shallowing-upward trends based on water depth estimates are less clear or obscured in part of the most proximal cores, possibly adding to the lack of separation between HST and TST samples in the ordinations (fig. 9*C*). The stratigraphic context becomes more discernible when analyses are restricted to an array of cores (e.g., cores 4, 5, and 6) parallel to the shoreline and equidistant to the depocenter (fig. 14*A*). In this case—and similar to the findings of Scarponi and Kowalewski (2004)—HST and TST samples ordinate consistent with their sequence stratigraphic interpretations (fig. 14*A*). Unlike the ordination pattern encompassing all samples (fig. 9*C*), sample DCA scores from the initial ordination plotted solely for cores 4–6 display TST samples with low to intermediate DC1 and DC2 scores. HST samples occur from intermediate to high DC1 and DC2 scores, demonstrating a noticeable separation between the HST and the TST. This separation indicates that cores sampled parallel to the coastline recover distal settings dominated by marine samples. In contrast, an ordination of a transverse transect of cores that include both proximal and distal settings produce ordination patterns where the separation between systems tracts becomes blurred (fig. 14*B*). Both TST and HST samples overlap across DC1 and DC2, as seen in figure 9*C*.

Although the Po Plain data set contains an extensive number of samples from different systems tracts and various depths, shallow-water HST samples dominate the data set (fig. 6). During the HST, net accumulation rates are relatively high and include more frequent depositional events compared with the other systems tracts of the Po Plain (Scarponi et al. 2013). The presence of numerous depositional events and thick sedimentary packages

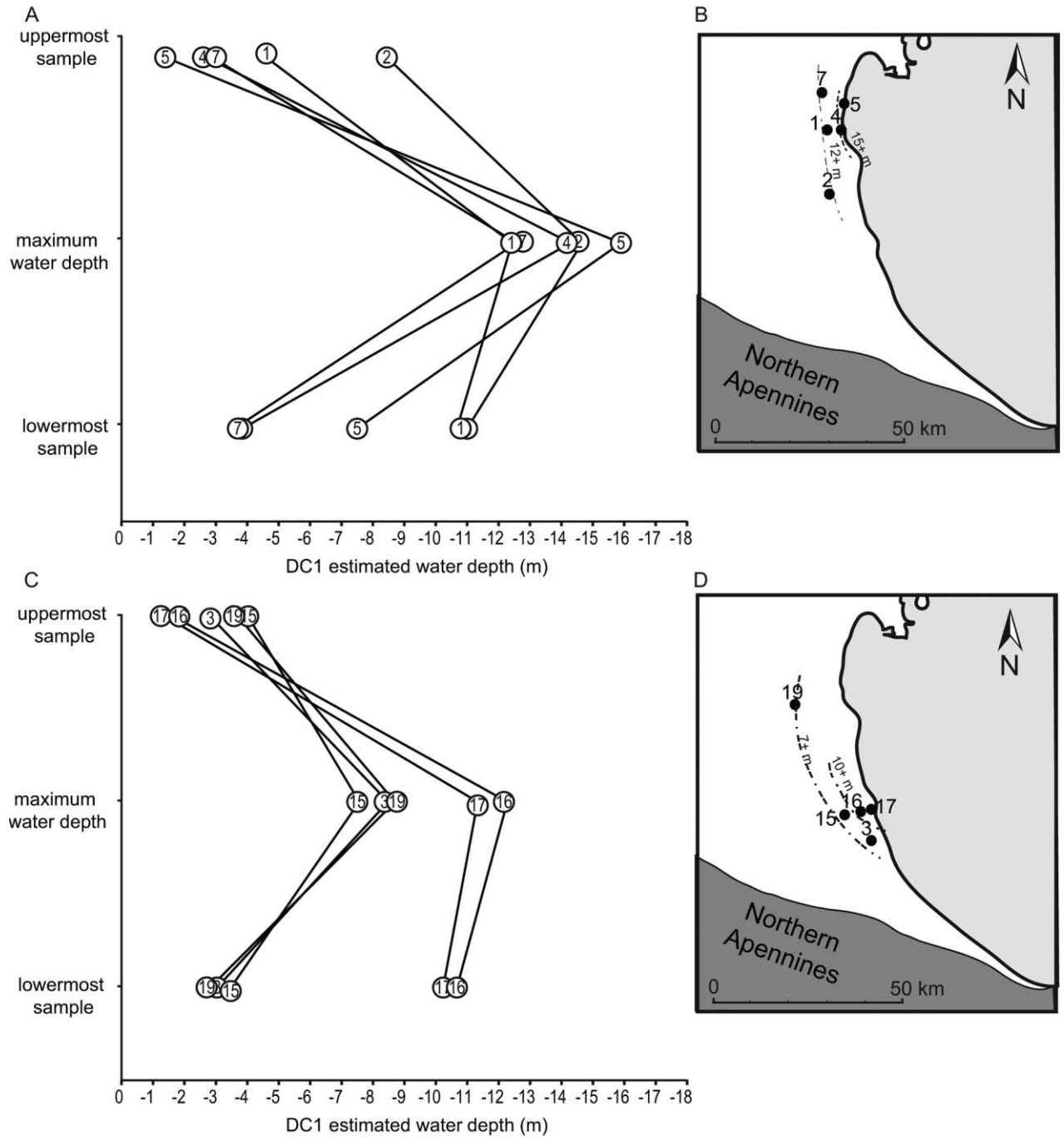

Figure 13. Comparison of maximum flooding zones and surfaces from S-DC-estimated depths for the Holocene. *A*, DC1-estimated maximum water depths plotted from seven northern cores. *B*, Map of northern Holocene cores and contour lines of their estimated maximum water depth. *C*, DC1-estimated maximum water depths plotted from five southern cores. *D*, Map of southern Holocene cores and contour lines of their estimated maximum water depth.

allow for an increased deposition and preservation of shallow-water fauna, possibly creating a bias in our data set for shallow-water samples. The dominance of shallow-water samples is consistent with recent modeling predictions of Holland and Christie (2013).

Despite the above-described caveats, bathymetric ordination models can potentially be applied to various stratigraphic and paleobiologic settings. Ordination models based on fossil assemblages can potentially improve estimates of bathymetric changes derived from facies analyses. The quanti-

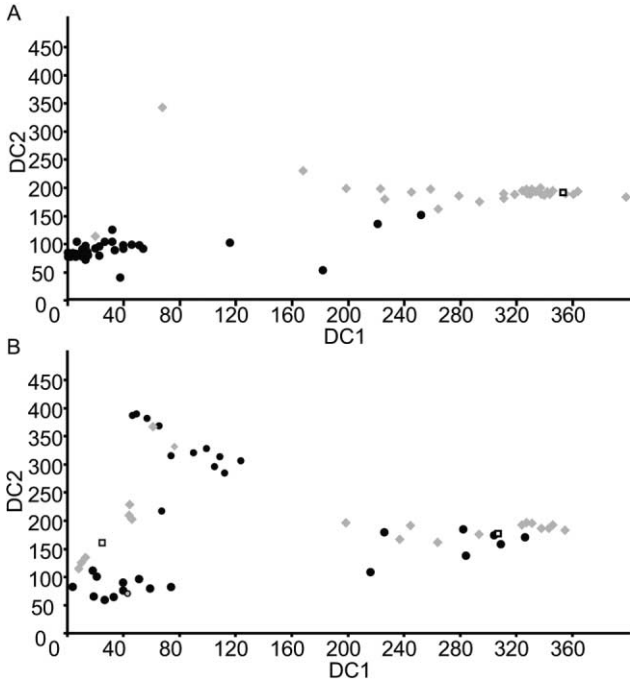

Figure 14. Detrended correspondence analysis of samples plotted by sequence stratigraphic interpretation. *A*, Parallel transect: cores 4, 5, and 6. *B*, Transverse transect: cores 6, 7, and 8. Gray diamonds indicate transgressive systems tract samples, black circles indicate highstand systems tract samples, the gray circle indicates a falling-stage systems tract sample, and white squares indicate maximum flooding surface/maximum flooding zone samples.

tative ordination-based approach can allow for environmentally better-resolved analyses of Pleistocene and Holocene communities and their response to relative sea-level changes. Origination, extinction, and turnover rates can be explored in more detail with respect to large-scale climatic, sea-level, and environmental changes. Finally, the approach enables tracking of onshore-offshore changes in the distribution of individual taxa.

The coupling of bathymetric models with stratigraphy allows for tracking of changes in relative sea level through time and space (Miller et al. 2001; Scarponi and Kowalewski 2004, 2007; Hendy 2013), a method that can be viewed as a natural extension of the coenocorrelation approach of Cisne and Rabe (1978; see also Springer and Bambach 1985). The previous models focused on preferred water depths of extant genera (EG) to quantify regional bathymetric gradients (Scarponi and Kowalewski 2004; Scarponi and Angeletti 2008; Hendy 2013). However, the multiordination approach proposed here allows for cross validation of different bathymetric models against each other and against the independently established sequence stratigraphic interpretations. Posteriori-calibrated sample depth estimates (S-DC) can be contrasted against estimated sample depth estimates (S-WA) to determine which model is most effective in explaining relative water levels. These models can be further applied to compare the direction of regional depositional gradients and flooding across the basin, particularly in the Quaternary because of well-known sea-level fluctuations. In addition, these models can aid in the development of paleobathymetric maps that can estimate quantitative changes in water depth. Paleobathymetric maps can show gradual deepening and shallowing-upward trends at multiple time slices to illustrate regional changes in environment and habitat within a given study area. Even in situations where environmental preferences for species cannot necessarily be estimated directly (i.e., the older fossil record dominated by species that lack closely related extant relatives), the composition of faunal assemblages can be modeled using ordination methods to improve stratigraphic interpretations (Cisne and Rabe 1978; Springer and Bambach 1985; Holland et al. 2001).

Conclusions

In this study, we have developed multiple quantitative ordination models to assess the regional bathymetry across a stratigraphically well-resolved area of the Po Basin (Italy). The ordination models were consistent in estimating water depth during the most recent geological history of the Po coastal plain and reaffirmed that multivariate analyses of fossil samples can (1) aid in evaluating high-resolution transgressive-regressive cycles by defining temporal water-level changes at fine resolution, (2) track maximum flooding across a basin by identifying maximum water depth through a three-dimensional network of cores, and (3) explore the spatial behavior of taxa by tracking their preferred depth distributions through time.

ACKNOWLEDGMENTS

We are grateful to J. Kerr, S. Langhi, S. Paskvich, A. Gomez, C. Haynes, and L. White for help with sample processing and specimen counts. We especially thank the New Technologies, Energy, and Environment Agency Santa Teresa Research Center for providing free access to the mollusk database. We also thank R. Pignone (Geological Survey of Regione Emilia-Romagna) and G. Gabbianelli (Dipartimento di Scienze Biologiche, Geologiche

e Ambientali) for providing access to the cores, and we thank M. Patzkowsky and one anonymous reviewer for their constructive comments, which improved this article considerably. This study was supported by National Foundation grant EAR-0920075, awarded to M. Kowalewski and D. Scarponi. Additional support via a Geological Society of America Student Research Grant and a ConocoPhillips Graduate Fellowship was provided to J. M. Wittmer.

REFERENCES CITED

Amorosi, A.; Bruno, L.; Rossi, V.; Severi, P.; and Hajdas, I. 2014*a*. Paleosol architecture of a late Quaternary basin-margin sequence and its implications for high-resolution, non-marine sequence stratigraphy. Global Planet. Change 111:12–25.

Amorosi, A.; Centineo, M. C.; Colalongo, M. L.; Pasini, G.; Sarti, G.; and Vaiani, S. C. 2003. Facies architecture and latest Pleistocene-Holocene depositional history of the Po Delta (Comacchio Area), Italy. J. Geol. 111:39–56.

Amorosi, A.; Colalongo, M. L.; Fiorini, F.; Fusco, F.; Pasini, G.; Vaiani, S. C.; and Sarti, G. 2004. Palaeogeographic and palaeoclimatic evolution of the Po Plain from 150-ky core records. Global Planet. Change 40:55–78.

Amorosi, A.; Colalongo, M. L.; Fusco, F.; Pasini, G.; and Fiorini, F. 1999. Glacio-eustatic control of continental–shallow marine cyclicity from late Quaternary deposits of the southeastern Po Plain, Northern Italy. Quat. Res. 52:1–13.

Amorosi, A.; Dinelli, E.; Rossi, V.; Vaiani, S. C.; and Sacchetto, M. 2008. Late Quaternary palaeoenvironmental evolution of the Adriatic coastal plain and the onset of Po River Delta. Palaeogeogr. Palaeoclimatol. Palaeoecol. 268:80–90.

Amorosi, A.; Rossi, V.; Scarponi, D.; Vaiani, S. C.; and Ghosh, A. 2014*b*. Biosedimentary record of postglacial coastal dynamics: high-resolution sequence stratigraphy from the northern Tuscan coast (Italy). Boreas 43:939–954.

Ayoub-Hannaa, W.; Huntley, J. W.; and Fürsich, F. T. 2013. Significance of detrended correspondence analysis (DCA) in palaeoecology and biostratigraphy: a case study from the Upper Cretaceous of Egypt. J. Afr. Earth Sci. 80:48–59.

Beals, E. W. 1984. Bray-Curtis ordination: an effective strategy for analysis of multivariate ecological data. Adv. Ecol. Res. 14:1–55.

Brett, C. E. 1995. Sequence stratigraphy, biostratigraphy, and taphonomy in shallow marine environments. Palaios 10:597–616.

Bush, A. M., and Brame, R. I. 2010. Multiple paleoecological controls on the composition of marine fossil assemblages from the Frasnian (Late Devonian) of Virginia, with a comparison of ordination methods. Paleobiology 36:573–591.

Carney, R. S. 2005. Zonation of deep biota on continental margins. Oceanogr. Mar. Biol. 43:211–278.

Ceregato, A.; Raffi, S.; and Scarponi D. 2007. The circalittoral/bathyal paleocommunities in the Middle Pliocene of northern Italy: the case of the *Korobkovia oblonga–Jupiteria concava* paleocommunity type. Geobios 40:555–572.

Cisne, J. L., and Rabe, B. D. 1978. Coenocorrelation: gradient analysis of fossil communities and its applications in stratigraphy. Lethaia 11:259–366.

Dattilo, B. F. 1996. A quantitative paleoecological approach to high-resolution cyclic and event stratigraphy: the Upper Ordivician Miamitown shale in the type Cincinnatian. Lethaia 29:21–37.

Emiliani, C. 1955. Pleistocene temperatures. J. Geol. 63:538–578.

———. 1966. Isotopic paleotemperatures. Science 154: 851–857.

Funder, S.; Demidov, I.; and Yelovicheva, Y. 2002. Hydrography and mollusc faunas of the Baltic and the White Sea–North Sea seaway in the Eemian. Palaeogeogr. Palaeoclimatol. Palaeoecol. 184:275–304.

Gauch, H. G. 1982. Multivariate analysis in community ecology. Cambridge Studies in Ecology. New York, Cambridge University Press, 298 p.

Gibbard, P. L. 2007. Climatostratigraphy. *In* Elias, S. A., ed. Encyclopedia of Quaternary science. Amsterdam, Elsevier, p. 2819–2825.

Greggio, N.; Mollema, P.; Antonellini, M.; and Gabbianelli, G. 2012. Irrigation management in coastal zones to prevent soil and groundwater salinization. *In* Abrol, V., ed. Resource management for sustainable agriculture. Rijeka, InTech. doi:10.5772/50534.

Grill, B., and Zuschin, M. 2001. Modern shallow- to deep-water bivalve death assemblages in the Red Sea—ecology and biogeography. Palaeogeogr. Palaeoclimatol. Palaeoecol. 16:75–96.

Gunderson, K.; Pazzaglia, F.; Anastasio, D.; Kodama, K.; Frankel, K.; Ponza, A.; Berti, C.; Smith, D.; Tanen, B.; and O'Neil M. 2011. Along-strike partitioning of shortening on thrust-related folds, Northern Apennine mountain front, Italy. Geophys. Res. Abstr. 13:5291.

Hammer, Ø.; Harper, D.; and Ryan, P. 2001. PAST: Paleontological statistics software for education and data analysis. Palaeontol. Electron. 4.

Hannon, J. S., and Meyer, D. L. 2014. Microendolithic structures from the Fort Payne Formation (lower Mississippian), Kentucky and Tennessee: implications for the paleoenvironment of carbonate mud-mounds. Palaeogeogr. Palaeoclimatol. Palaeoecol. 393:20–29.

Hendy, A. J. W. 2013. Spatial and stratigraphic variation of marine paleoenvironments in the middle-upper Miocene Gatun Formation, Isthmus of Panama. Palaios 28:210–227.

Hendy, A. J. W., and Kamp, P. J. J. 2007. Paleoecology of late Miocene–early Pliocene sixth-order glacioeustatic sequences in the Manutahi-1 core, Wanganui-Taranaki Basin, New Zealand. Palaios 22:325–337.

Hill, M. O. 1973. Reciprocal averaging: an eigenvector method of ordination. J. Ecol. 61:237–249.

Hill, M. O., and Gauch, H. G. 1980. Detrended correspondence analysis: an improved ordination technique. Vegetatio 42:47–58.

Holland, S. M. 1995. The stratigraphic distribution of fossils. Paleobiology 21:92–109.

———. 2000. The quality of the fossil record—a sequence stratigraphic perspective. *In* Erwin, D. H., and Wings, S. L., eds. Deep time: paleobiology's perspective. Lawrence, KS, Paleontological Society, p. 148–168.

———. 2005. The signatures of patches and gradients in ecological ordinations. Palaios 20:573–580.

Holland, S. M., and Christie, M. 2013. Changes in area of shallow siliciclastic marine habitat in response to sediment deposition: implications for onshore-offshore paleobiologic patterns. Paleobiology 39:511–524.

Holland, S. M.; Miller, A. I.; Meyer, D. L.; and Dattilo, B. F. 2001. The detection and importance of subtle biofacies within a single lithofacies: the Upper Ordovician Kope Formation of the Cincinnati, Ohio region. Palaios 16:205–217.

Holland, S. M., and Patzkowsky, M. E. 2007. Gradient ecology of a biotic invasion: biofacies of the type Cincinnatian series (Upper Ordovician), Cincinnati, Ohio region, USA. Palaios 22:392–407.

Huntley, J. W., and Scarponi, D. 2012. Evolutionary and ecological implications of trematode parasitism of modern and fossil northern Adriatic bivalves. Paleobiology 38:40–51.

Ivany, L. C.; Brett, C. E.; Wall, H. L. B.; Wall, P. D.; and Handley, J. C. 2009. Relative taxonomic and ecologic stability in Devonian marine faunas of New York State: a test of coordinated stasis. Paleobiology 35: 499–524.

Jackson, D. A., and Somers, K. M. 1991. Putting things in order: the ups and downs of detrended correspondence analysis. Am. Nat. 137:704–712.

Kenkel, N. C., and Orlóci, L. 1986. Applying metric and nonmetric multidimensional scaling to ecological studies: some new results. Ecology 67:919–928.

Konar, B.; Iken, K.; and Edwards, M. 2008. Depth-stratified community zonation patterns on Gulf of Alaska rocky shores. Marine Ecology 30:63–73.

Kowalewski, M.; Gürs, K.; Nebelsick, J. H.; Oschmann, W.; Piller, W. E.; and Hoffmeister, A. P. 2002. Multivariate hierarchical analyses of Miocene mollusk assemblages of Europe: paleogeographic, paleoecological, and biostratigraphic implications. Geological Society of America Bulletin 114:239–256.

Lafferty, A.; Miller, A. I.; and Brett, C. E. 1994. Comparative spatial variability in faunal composition along two Middle Devonian paleoenvironmental gradients. Palaios 9:224–236.

McCune, B., and Grace, J. B. 2002. Analysis of ecological communities. Gleneden Beach, OR, MjM Software, 304 p.

Miller, A. I.; Holland, S. M.; Meyer, D. L.; and Dattilo, B. F. 2001. The use of faunal gradient analysis for intraregional correlation and assessment of changes in sea-floor topography in the type Cincinnatian. J. Geol. 109:603–613.

Minchin, P. R. 1987. An evaluation of the relative robustness of techniques for ecological ordination. Vegetatio 69:89–107.

Muttoni, G.; Ravazzi, C.; Breda, M.; Laj, C.; Kissel, C.; Mazaud, A.; Pini, R.; and Garzanti, E. 2007. Magnetostratigraphic dating of an intensification of glacial activity in the southern Italian Alps during marine isotope stage 22. Quat. Res. 67:161–173.

Olabarria, C. 2006. Faunal change and bathymetric diversity gradient in deep-sea prosobranchs from northeastern Atlantic. Biodivers. Conserv. 15:3685–3702.

Olszewski, T. D., and Patzkowsky, M. E. 2001. Measuring recurrence of marine biotic gradients: a case study from the Pennsylvanian-Permian midcontinent. Palaios 16:444–460.

Patzkowsky, M. E., and Holland, S. M. 1996. Extinction, invasion, and sequence stratigraphy: patterns of faunal change in the Middle and Upper Ordovician of the eastern United States. *In* Witzke, B. J.; Ludvigson, G. A.; and Day, J. E., eds. Paleozoic sequence stratigraphy: views from the North American Craton. Geol. Soc. Am. Spec. Pap. 306:131–142.

———. 2012. Stratigraphic paleobiology: understanding the distribution of fossil taxa in time and space. Chicago, University of Chicago Press, 259 p.

Peters, S. E. 2005. Geologic constraints on the macroevolutionary history of marine animals. Proc. Natl. Acad. Sci. U.S.A. 102:12326–12331.

———. 2006. Genus extinction, origination, and the duration of sedimentary hiatuses. Paleobiology 32:387–407.

Peters, S. E., and Heim, N. A. 2010. The geological completeness of paleontological sampling in North America. Paleobiology 36:61–79.

Pieri, M., and Groppi, G. 1981. Subsurface geological structure of the Po Plain, Italy. Rome, Consiglio Nazionale delle Ricerche, 23 p.

Redman, C. M.; Leighton, L. R.; Schellenberg, S. A.; Gale, C. N.; Nielsen, J. L.; Dressler, D. L.; and Klinger, M. K. 2007. Influence of spatiotemporal scale on the interpretation of paleocommunity structure: lateral variation in the Imperial Formation of California. Palaios 22:630–641.

SAS Institute. 2002. SAS/IML software, ver. 9.0. Cary, NC, SAS Institute, 501 p.

Scarponi, D., and Angeletti, L. 2008. Integration of palaeontological patterns in the sequence stratigraphy paradigm: a case study from Holocene deposits of the Po Plain (Italy). GeoActa 7:1–13.

Scarponi, D.; Huntley, J. W.; Capraro, L.; and Raffi, S. 2014. Stratigraphic paleoecology of the Valle di

Manche section (Crotone Basin, Italy): a candidate GSSP of the Middle Pleistocene. Palaeogeogr. Palaeoclimatol. Palaeoecol. 402:30–43.

Scarponi, D.; Kaufman, D.; Amorosi, A.; and Kowalewski, M. 2013. Sequence stratigraphy and the resolution of the fossil record. Geology 41:239–242.

Scarponi, D., and Kowalewski, M. 2004. Stratigraphic paleoecology: bathymetric signatures and sequence overprint of mollusk associations from upper Quaternary sequences of the Po Plain, Italy. Geology 32:989–992.

———. 2007. Sequence stratigraphic anatomy of diversity patterns: Late Quaternary benthic mollusks of the Po Plain, Italy. Palaios 22:296–305.

Smale, A. B. 2008. Continuous benthic community change along a depth gradient in antarctic shallows: evidence of patchiness but not zonation. Polar Biol. 31:189–198.

Smrecak, T. A. 2008. Toward an epibiofacies model: a comparison of depth-related epibiont gradients in the Cincinnatian (Late Ordovician) and present-day. MS thesis, University of Cincinnati, Cincinnati, OH.

Springer, D. A., and Bambach, R. K. 1985. Gradient versus cluster analysis of fossil assemblages: a comparison from the Ordovician of southwestern Virginia. Lethaia 18:181–198.

Wartenberg, D.; Ferson, S.; and Rohlf, F. J. 1987. Putting things in order: a critique of detrended correspondence analysis. Am. Nat. 129:434–448.

Zong, Y., and Horton, B. P. 1999. Diatom-based tidal-level transfer functions as an aid in reconstructing Quaternary history of sea-level movements in the U.K. J. Quat. Sci. 14:153–167.

Zuschin, M.; Harzhauser, M.; Hengst, B.; Mandic, O.; and Roetzel, R. 2014. Long-term ecosystem stability in an Early Miocene estuary. Geology 42:7–10.

Zuschin, M.; Harzhauser, M.; and Mandic, O. 2007. The stratigraphic and sedimentologic framework of fine-scale faunal replacements in the middle Miocene of the Vienna Basin (Austria). Palaios 22:285–295.

———. 2011. Disentangling palaeodiversity signals from a biased sedimentary record: an example from the Early to Middle Miocene of Central Paratethys Sea. *In* McGowan, A. J., and Smith, A. B., eds. Comparing the geological and fossil records: implications for biodiversity studies. Geol. Soc. Spec. Publ. 358: 123–139.